Weierstraß-Institut
für Angewandte Analysis und Stochastik

im Forschungsverbund Berlin e. V.

Preprint ISSN 2198 – 5855

Anisotropy in wavelet based phase field models

Maciek D. Korzec[1], Andreas Münch[2], Endre Süli [3], Barbara Wagner[1,4]

submitted: December 16, 2014

[1] Institute of Mathematics
Technische Universität Berlin
Str. des 17. Juni 136
10623 Berlin
Germany
E-Mail: korzec@math.tu-berlin.de

[2] Mathematical Institute
24-29 St Giles'
University of Oxford
Oxford, OX1 3LB
UK
E-Mail: muench@maths.ox.ac.uk

[3] Mathematical Institute
24-29 St Giles'
University of Oxford
Oxford, OX1 3LB, UK
E-Mail: endre.suli@maths.ox.ac.uk

[4] Weierstrass Institute
Mohrenstr. 39
10117 Berlin
Germany
E-Mail: barbara.wagner@wias-berlin.de

No. 2050
Berlin 2014

2010 *Mathematics Subject Classification.* 34E13, 74N20, 74E10.

Key words and phrases. Phase-field model, wavelets, sharp interface model, free boundaries.

This publication was based on work supported in part by Award No KUK-C1-013-04, made by King Abdullah University of Science and Technology (KAUST). MK and BW acknowledges additional support by the DFG MATHEON research centre, within project C10 and the Federal Ministry of Education (BMBF) and the state government of Berlin (SENBWF) in the framework of the program *Spitzenforschung und Innovation in den Neuen Ländern* (Grant Number 03IS2151).

Edited by
Weierstraß-Institut für Angewandte Analysis und Stochastik (WIAS)
Mohrenstraße 39
10117 Berlin
Germany

Fax: +49 30 2044975
E-Mail: preprint@wias-berlin.de
World Wide Web: http://www.wias-berlin.de/

Abstract

Anisotropy is an essential feature of phase-field models, in particular when describing the evolution of microstructures in solids. The symmetries of the crystalline phases are reflected in the interfacial energy by introducing corresponding directional dependencies in the gradient energy coefficients, which multiply the highest order derivative in the phase-field model. This paper instead considers an alternative approach, where the anisotropic gradient energy terms are replaced by a wavelet analogue that is intrinsically anisotropic and linear. In our studies we focus on the classical coupled temperature - Ginzburg-Landau type phase-field model for dendritic growth. For the resulting derivative-free wavelet analogue existence, uniqueness and continuous dependence on initial data for weak solutions is proved. The ability to capture dendritic growth similar to the results obtained from classical models is investigated numerically.

1 Introduction

Since at least the late 1980s, wavelets have been the focus of intensive research and have developed into an indispensable tool for signal and image processing. Wavelet compression is used, for example, in the JPEG2000 image compression standard. From the vast literature on the mathematical theory of wavelets, we mention only the ten lectures by Daubechies [7] which provide a classical introduction to the field and a more recent overview by Mallat [18]. Wavelets have also been explored for their use in numerical approximation of PDEs and operator equations [6], through Galerkin type methods [14], in wavelet collocation methods [21, 22] or as a tool to determine sparse grids for other common discretisation methods [5, 13, 15, 19].

A completely new role of wavelets in the context of PDEs has recently been introduced by Dobrosotskaya and Bertozzi [8–10] in applications from image processing. The key idea is to replace the differential operators in a Ginzburg-Landau free energy formulation by a pseudo-differential operator defined in wavelet space so that a Besov or Besov type semi-norm is used instead of the “square-gradient” H^1 semi-norm. In the Euler-Lagrange or steepest gradient descent equation the Laplacian is correspondingly replaced by a wavelet analogue. The new approach, intended to improve results for sharper image reconstructions, also introduced anisotropy of the solutions with a four- or eight-fold symmetry. In particular, the authors determined and proved the Γ-limit for the new energy [2, 9] and showed that it exhibits a square anisotropy of Wulff shape [4, 12, 25], as well as that the “derivative-free” wavelet analogue of the Allen-Cahn equation is well posed [10]. In the work presented here, we will make use of this idea for modeling the anisotropic patterns that typically arise in the evolution of microstructure in solids.

An area where anisotropy is essential is crystal growth and solidification. Many aspects of solidification and crystal growth has been well studied throughout the last decades, the large literature and remeining open problems in this research field can be found in the review by e.g. Glicksman [11]. One of the most widely studied model equations of dendritic recrystallisation goes back to Kobayashi's work [17] which introduces a phase-field model where the gradient terms has an anisotropic weight γ that depends on the spatial gradient of the phase-field variable ∇u, specifically, a function of the angle θ between the direction of ∇u and a reference direction, usually taken to be the x-axis. A choice typically used in the literature for the interface energy, that will also be used here, is $\gamma(\theta) = 1 + \delta \cos(n\theta)$, where $n > 0$ is an integer parameter that leads to an n-fold symmetry and $\delta \geq 0$ is chosen so that for weak to moderate anisotropy $\gamma(\theta) + \gamma''(\theta)$ (with $' = d/d\theta$) is strictly positive for all θ.

This type of anisotropic weighting of the gradients has been extensively investigated, e.g. [16, 24], also as part of models using coupled systems of PDES, for which for example existence of solutions was shown in [3]. The model has also been used to develop and improve numerical methods, starting with Kobayashi's own work [17]. Recently a study on a finite element method applied to a very similar model has been carried out [1], which in addition to describing a stable scheme also gives and overview of various numerical approaches for phase-field models and their sharp interface limits.

Here, we introduce instead for the leading order derivative a wavelet analogue along the lines of Dobrosotskaya and Bertozzi [8–10]. We show that the new model of capturing dendritic growth similar to Kobayashi's original model for the case of a four-fold symmetry. While the latter is nonlinear in the highest derivative terms, the proposed model is derivative free in the phase-field variable. The new wavelet term is linear and has a simple form in wavelet space similar to the diagonal representation of differential operators in Fourier space. As a consequence, the mathematical analysis as well as numerical approaches for the new PDE' models are expected to simplify.

The paper is structured as follows. We begin with a formulation of both models in Section 2, where we also summarise the essential notions about wavelets and Besov-type norms and also define the wavelet analogue Laplacian that we use. In section 3, we prove well-posedness, in particular existence and uniqueness.

Results from numerical experiments that systematically explore the evolution of anisotropy in these models and comparisons to the results of classical models are discussed in section 4. Starting with limiting and simpler special case, the anisotropic Allen-Cahn equation, we first investigate the different scaling behaviours of the evolution the original anisotropic Allen-Cahn and its wavelet analogue. Then for the full recrystallisation model the dendritic morphologies are dicussed. Finally, in section 5, we summarise our conclusions and give an outlook on implications and further directions of research. The generality of the new modelling paradigm will be discussed throughout this work.

2 Dendritic recrystallisation: A wavelet-based model

Kobayashi [17] introduced a model that couples an anisotropic phase-field with a heat equation to describe recrystallisation from a melt and the evolution of dendritic pat-

terns similar to those observed in experiments. We have two fields, the phase field $u(\boldsymbol{x}, t)$ which is 0 and 1 in the pure liquid and solid phase, respectively, and the temperature field $T(\boldsymbol{x}, t)$, where $\boldsymbol{x} = (x, y) \in \Omega \equiv [0, 1]^2$ are the spatial variables and t denotes time. For simplicity, we assume u and T to be 1-periodic in both x and y. The evolution of the phase-field is given by a Ginzburg-Landau equation which follows from the L^2 gradient flow $\tau u_t = -\delta\mathcal{E}/\delta u$ of the free energy

$$\mathcal{E} = \mathcal{E}(u; A, \varepsilon, m) = \int \frac{\varepsilon}{2}\gamma(\theta)^2|\nabla u|^2 + \frac{1}{\varepsilon}W(u; m)d\Omega\,, \tag{1}$$

with the homogeneous free energy contribution

$$W(u; m) = \frac{1}{4}u^2(u-1)^2 + m\left(\frac{1}{3}u^3 - \frac{1}{2}u^2\right)\,. \tag{2}$$

and the positive parameter $\varepsilon \ll 1$ that controls the width of the interface layer. The variable $\theta = \text{atan2}(u_x, y_y)$ denotes the angle between the gradient of u and the x axis, unless the gradient is zero, in which case we let $\theta = 0$. For an isotropic system γ is set to a constant, while in this paper, we typically consider a four-fold symmetry by setting a specific choice for the interface energy

$$\gamma(\theta) = 1 + \delta\cos(n\theta) \tag{3}$$

with $n = 4$, and where for weak to moderate accuracy $\delta > 0$ is chosen so that $\gamma(\theta) + \gamma''(\theta)$ (with $' = d/d\theta$) is strictly positive for all θ. Thus, we have

$$\tau u_t = -\varepsilon\frac{\partial}{\partial_x}(\gamma\gamma'\frac{\partial}{\partial y}u) + \varepsilon\frac{\partial}{\partial_y}(\gamma\gamma'\frac{\partial}{\partial x}u) + \varepsilon\nabla(\gamma^2\nabla u) + \frac{1}{\varepsilon}W'(u; m)\,, \tag{4}$$

where τ is a time scale (a small positive constant). This equation is coupled to the heat equation for the temperature T

$$T_t = c\Delta T + Ku_t\,, \tag{5}$$

by the dimensionless parameter K which determines the latent heat contribution from the phase change at the interface, and by letting m depend on the temperature

$$m(T) = \frac{c_1}{\pi}\arctan(c_2(T_e - T)) \tag{6}$$

as in Kobayashi's work. Notice that W and m have been carefully chosen so that the W is always a double-well potential with minima occurring at $u = 0$ and $u = 1$ if $c_1 < 1$, so that energy production or dissipation is negligible for pure phase and therefore away from interfaces.

For the new wavelet-based model, we replace the gradient term with the nonlinear factor by the Besov-type semi-norm,

$$\mathcal{E}(u; B, \varepsilon, m) = \frac{\varepsilon}{2}|u|_B^2 + \int \frac{1}{\varepsilon}W(u; m)d\Omega\,. \tag{7}$$

so that the L^2 gradient flow is now given by

$$\tau u_t = \varepsilon\Delta_w u - \frac{1}{\varepsilon}W_u(u; m)\,, \tag{8a}$$

where Δ_w is a wavelet analogue of the Laplacian, while the heat equation remains unchanged,

$$T_t = c\Delta T + Ku_t\,. \tag{8b}$$

The construction of $|\cdot|_B$ and Δ_w follows the work by Dobrosotskaya and Bertozzi and for convenience to the reader it is summarised in the appendix A.

Remark Before we will show existence, uniqueness and well-posedness of the new model (8) we like to point out some observations concerning thermodynamical consistency of phase-field models. We begin with the introduction of the entropy functional S based on its entropy density s

$$S = \int s d\Omega = \int \frac{e-F}{\vartheta} d\Omega\,. \tag{9}$$

Here, ϑ is the absolute temperature, F is the free energy and e is the internal energy density,

$$e = c_p\vartheta + L(1-u)\,, \tag{10}$$

with the specific heat c_p and enthalpy of fusion L, see for example [20]. For the free energy we exploit the wavelet semi-norm, as F is given implicitly by the following expression

$$\int F(u)d\Omega = \frac{\varepsilon}{2}|u|_B^2 + \frac{1}{\varepsilon}\int W(u;m)d\Omega\,. \tag{11}$$

For now we assume that W is defined as in (2), however, we set $m = 6\frac{\vartheta-\vartheta_m}{\vartheta_m}$ and ϑ_m is the melting temperature. The principle of entropy production then leads to the coupled evolution equations

$$\tau u_t = -\frac{\delta}{\delta u}\int F d\Omega = \varepsilon\Delta_w u - \frac{1}{\varepsilon}W'(u;m) \tag{12}$$

$$e_t = -\nabla M\nabla\frac{\delta}{\delta e}\int \frac{e}{\vartheta}d\Omega = -\nabla M\nabla\frac{1}{\vartheta} = \nabla\frac{M}{\vartheta^2}\nabla\vartheta\,. \tag{13}$$

By setting $M = c_p\vartheta^2, T = \vartheta/\vartheta_m$ and insertion of (10) into the second equation one deduces

$$\tau u_t = \varepsilon\Delta_w u - \frac{1}{\varepsilon}\left(-u^3 + \frac{3}{2}u^2 - \frac{1}{2}u) + 6(T-1)(u-u^2)\right) \tag{14}$$

$$\frac{1}{\theta_m^2}T_t = Ku_t + \nabla^2 T\,. \tag{15}$$

We expressed the system in terms of the nondimensional temperature T and used $K = L/(c_p\vartheta_m^2)$, $\tilde{\tau} = 1/\theta_m^2$. In the following simulations we will use a different form of m as it has been proposed by Kobayashi [17]. He introduced the nonlinearity $m(T) = \frac{\alpha}{\pi}\arctan(\beta(T-T_e))$. Here, with the nondimensional critical temperature $T_e = 1$ one chooses $\beta > 0$ and $\alpha < 1$ to guarantee that $|m(T)| < 1/2$ and hence that the double-wells always have two pronounced minima. Such a form of the energy density is valid near the T_e. In fact, near this temperature we have $m(1+T) = m(1) + m'(1)T$+higher order terms. Hence, $m(\tilde{T}+1) = \frac{\alpha}{\pi}\beta\tilde{T}$+higher order terms. Choosing $T = \tilde{T}+1$ and $\frac{\alpha}{\pi}\beta = 6$, this is indeed as above, hence the nonlinear version is still a thermodynamically valid choice in the linearised sense. However, to prove this for the nonlinear model would not be straightforward, as has been discussed by Wang et al. [23] for the original model by Kobayashi.

3 Well-posedness of the wavelet based model

As an important prerequisite for sensible numerical simulations using the new wavelet-based model, we first prove existence, uniqueness and continuous dependence on initial data for weak solutions of the system (8), with initial conditions $u(x,0) = u_0(x)$, $T(x,0) = T_0(x)$, where we allow for $\Omega = [0,1]^d$ to be either two or three dimensional, with u and T being 1-periodic in all spatial directions. (In this section, we use a simplified notation that does not distinguish between vectors and scalars.)

The results are formulated for the Sobolev space $H_p^m(\Omega)$, $m \in \mathbb{N}$, which denotes all $f \in H_{loc}^m(\mathbb{R}^n)$ that are 1-periodic in all spatial directions and which is equipped with the usual inner product and norm, given by

$$(u,v)_{H^m} = \sum_{|\kappa|\leq m} \int_\Omega D^\kappa u(x) D^\kappa v(x) dx, \quad \|u\|_{H^m} = \sqrt{(u,u)_{H^m}}\,,$$

in multi-index notation. In the following, C is used for generic constants that do not depend on the relevant quantities. In contrast to Kobayashi's model, for which proving well-posedness is quite intricate (see for example [3]), this is relatively straightforward for the new model and essentially combines a Galerkin approach and with repeated use of the equivalence of relevant semi-norms.

Theorem 1 (Existence of weak solutions)**.** *Let $(u_0, T_0) \in H_p^1 \cap L_p^4 \times H_p^1$, then the above problem defined via r-regular wavelets with $r \geq 2$ has a weak solution with*

$$\begin{aligned} u &\in L^\infty(0,\bar{t}; H_p^1 \cap L_p^4) \cap L^2(0,\bar{t}; H_p^2) \\ T &\in L^\infty(0,\bar{t}; H_p^1) \cap L^2(0,\bar{t}; H_p^2) \end{aligned}$$

and

$$u_t \in L^2(0,\bar{t}; L_p^2), \quad T_t \in L^2(0,\bar{t}; L_p^2)\,.$$

Proof. To work with weak solutions, we introduce as in reference [10] the bilinear operator $\mathcal{B} : H_p^1 \times H_p^1 \to \mathbb{R}$ with

$$\mathcal{B}(u,v) = \lim_{n\to\infty} (\Delta_w u_n, v)\,,$$

where $u, v \in H_p^1$ and (u_n) is a set of H_p^2 functions converging to u in H_p^1. With this operator we write and use the following weak form

$$(u_t, \varphi) = \varepsilon \mathcal{B}(u,\varphi) - \frac{1}{\varepsilon}(W_u(u;m), \varphi) \tag{16}$$

$$(T_t, \phi) = -c(\nabla T, \nabla \phi) + K(u_t, \phi), \quad \varphi, \phi \in H_p^1\,, \tag{17}$$

with $m(t) = \frac{c_1}{\pi} \arctan(c_2(T_e - T(t))), c_1 < 1\,.$

For the Galerkin approximation we insert $u^n = \sum_{j=0}^n b_j \varphi_j(x), T^n = \sum_{j=0}^n d_j \varphi_j(x)$, where the set $\{\varphi_j\}_j$ forms an orthonormal basis of H_p^1 – say the smooth eigenfunction of the Laplacian on the periodic Torus. Then we treat the weak form in terms of the

basis functions

$$(u_t^n, \varphi_k) = \varepsilon \mathcal{B}(u^n, \varphi_k) - \frac{1}{\varepsilon}(W_u(u^n; m^n), \varphi_k) \tag{18}$$

$$(T_t^n, \varphi_k) = -c(\nabla T^n, \nabla \varphi_k) + K(u_t^n, \varphi_k) \tag{19}$$

$$(u^n, \varphi_k) = \xi_k \tag{20}$$

$$(T^n, \varphi_k) = \eta_k, \quad k = 0, \ldots, n\,. \tag{21}$$

with $m^n(t) = \frac{c_1}{\pi}\arctan(c_2(T_e - T^n(t))), c_1 < 1$. Here $\xi_k = \xi_k(n)$ are such that

$$\sum_{j=0}^{n} \xi_j \varphi_j \to u_0, \text{ in } H_p^1 \cap L_p^4\,,$$

as $n \to \infty$, and for $\eta_k(n)$

$$\sum_{j=0}^{n} \eta_j \varphi_j \to T_0, \text{ in } H_p^1\,.$$

As φ_j are a basis of the above spaces and as $u_0 \in H_p^1 \cap L_p^4, T_0 \in H_p^1$, such coefficients do exist. Due to the orthogonality of the basis functions we obtain an ODE system for the coefficients whose system function is locally Lipschitz due to the boundedness of the $\mathcal{B}$ operator. This gives local existence.

We obtain bounds for the Galerkin approximation and then pass to the limit. Therefore we drop the n notation and keep in mind to work with the finite dimensional approximation until the limiting process is mentioned. As m stays bounded between $-1/2$ and $1/2$, with a properly chosen small constant $C > 0$ next to the double-well $W(u; m)$ also the function $\tilde{W}(u; m) = W_u(u; m)u$ is bounded. In particular we will use that $W > -C > -0.2$ and the same kind of bound for $\tilde{W}$.

Testing equation (16) by u yields

$$\frac{1}{2}\frac{d}{dt}\|u\|^2 + \varepsilon |u|_B^2 = -\frac{1}{\varepsilon}(W_u(u; m), u)$$

as we can use in the Galerkin approximation that $\mathcal{B}(u, u) = (\Delta_w u, u) = -|u|_B^2$ (see e.g. [10]).

The second term reads, noting that by the choice of $c_1 < 1$ we can use $m \in [-\frac{1}{2} + \delta, \frac{1}{2} - \delta]$ for some small number $\delta \ll 1$.

$$-\frac{1}{\varepsilon}\int W_u(u; m) u dx \leq \frac{1}{\varepsilon}\int -u^4 + (2-\delta)u^2|u| + (m - \frac{1}{2})u^2 dx \leq \frac{1}{2\varepsilon}(-\|u\|^4 + 2\|u\|^2)\,.$$

We used that $(\int u^2)^2 \leq \|u^2\|^2\|1\|^2 = \int u^4 dx$. Hence if $\|u\| > \sqrt{2}$, $d/dt\|u\|$ is decreasing, independently of the value of m (with more care one could derive a smaller bound). We established a uniform bound for the L^2 norm

$$\|u\| \leq \max\{\sqrt{2}, \|u_0\|\}\,.$$

Additionally as $(-\|u\|^4 + 2\|u\|^2) \leq 1$ we get the $\bar{t}$ dependent bound, after integrating over $[0, \bar{t}]$,

$$\frac{1}{2}\|u(\bar{t})\|^2 + \int_0^{\bar{t}} \varepsilon |u|_B^2 dt \leq \frac{1}{2}\|u_0\|^2 + \bar{t}/(2\varepsilon)\,.$$

As the B semi-norm is equivalent to the Besov $B^1_{2,2}$ semi-norm for sufficiently regular wavelets, it is equivalent to the H^1 semi-norm, see the discussions and references in the papers by Dobrosotskaya and Bertozzi [8, 10]. Due to this equivalence we obtain $\int_0^{\bar{t}} \varepsilon |u|^2_{H^1_p} dt \leq C + \bar{t}/(2\varepsilon)$, and hence one has for any fixed $\bar{t}$

$$u \in L^\infty(0, \bar{t}; L^2_p(\Omega)), \quad u \in L^2(0, \bar{t}; H^1_p(\Omega)) \,.$$

Testing equation (16) by u_t gives

$$\|u_t\|^2 = -\frac{\varepsilon}{2}\frac{d}{dt}|u|^2_B - \frac{1}{\varepsilon}(W_u(u;m), u_t) \,. \tag{22}$$

Integrating over time $[0, \bar{t}]$ yields

$$\int_0^{\bar{t}} \|u_t\|^2 dt + \frac{\varepsilon}{2}|u(\bar{t})|^2_B = \varepsilon |u(0)|^2_B - \frac{1}{\varepsilon}\int_0^{\bar{t}} (W_u(u;m), u_t) dt \,.$$

The term to control on the right hand side is

$$\begin{aligned} -\frac{1}{\varepsilon}\int_0^{\bar{t}} (W_u(u;m), u_t) dt &\leq -\frac{1}{4\varepsilon}\int_0^{\bar{t}} \frac{d}{dt}\|u\|_4^4 dt + \frac{1}{\varepsilon}\int_0^{\bar{t}} (2u^2, |u_t|) + (|u|, |u_t|) dt \\ &\leq -\frac{1}{4\varepsilon}(\|u(\bar{t})\|_4^4 - \|u(0)\|_4^4) + \frac{4}{\varepsilon^2}\int_0^{\bar{t}} \|u\|_4^4 dt \\ &+ \frac{1}{2}\int_0^{\bar{t}} \|u_t\|^2 dt + \frac{1}{\varepsilon^2}\int_0^{\bar{t}} \|u\|^2 dt \,. \end{aligned}$$

Using the L^2 bound on u, inserting into (22) and rearranging yields

$$\frac{1}{2}\int_0^{\bar{t}} \|u_t\|^2 dt + \varepsilon |u(\bar{t})|^2_B + \frac{1}{4\varepsilon}\|u(\bar{t})\|_4^4 \leq C(\bar{t}) + \frac{4}{\varepsilon^2}\int_0^{\bar{t}} \|u\|_4^4 dt \,.$$

In particular we have derived, with $F(t) = \|u(t)\|_4^4$,

$$F(\bar{t}) \leq C(\bar{t}, \varepsilon) + \frac{16}{\varepsilon}\int_0^{\bar{t}} F(t) dt \,.$$

Gronwall's inequality states, as C is non-decreasing in $\bar{t}$, that

$$F(\bar{t}) \leq C(\bar{t}, \varepsilon) e^{\int_0^{\bar{t}} \frac{4}{\varepsilon} dt} = C(\bar{t}, \varepsilon) e^{\frac{4\bar{t}}{\varepsilon}} = \tilde{C}(\bar{t}, \varepsilon) \,.$$

This is a bound growing exponentially fast with $\bar{t}$, but this is sufficient to overall conclude that

$$u \in L^2(0, \bar{t}; L^4_p(\Omega)), \quad u_t \in L^2(0, \bar{t}; L^2_p(\Omega)) \tag{23}$$

and as due to the equivalence of the semi-norms we have $a|u(\bar{t})|_{H^1} \leq |u(\bar{t})|_B$, we conclude further with the bound

$$u \in L^\infty(0, \bar{t}; H^1_p(\Omega)) \,.$$

Now we need to establish useful bounds for the temperature. Testing (17) by T_t leads to

$$\|T_t\|^2 + \frac{c}{2}\frac{d}{dt}|T|^2_{H^1} = K(u_t, T_t) \leq \frac{K^2}{2}\|u_t\|^2 + \frac{1}{2}\|T_t\|^2 \,. \tag{24}$$

Integrating over time yields, using (23),

$$\int_0^{\bar{t}} \|T_t\|^2 dt + c|T(\bar{t})|_{H^1}^2 \leq C(T(0), \bar{t}, K) \tag{25}$$

and

$$T \in L^\infty(0, \bar{t}; H_p^1(\Omega)), \quad T_t \in L^2(0, \bar{t}; L_p^2(\Omega)) \,.$$

To obtain a higher order bound we test with $-\Delta u$ and we obtain

$$\begin{aligned}
\frac{d}{dt}|u|_{H^1}^2 &= \varepsilon(\Delta_w \nabla u, \nabla u) + \frac{1}{\varepsilon}\int W_u(u;m)\Delta u dx \\
&\leq -\varepsilon|\nabla u|_B^2 + C(\varepsilon, \bar{\varepsilon})\int u^6 dx + \frac{\varepsilon\bar{\varepsilon}}{2}|\nabla u|_{H^1}^2 \\
&\leq -\tilde{C}|\nabla u|_{H^1}^2 + C\|u\|_{H^1}^6 \,.
\end{aligned}$$

Here we used a small $\bar{\varepsilon}$ to get rid of the second order term with the wrong sign. As $u \in L^\infty(0, \bar{t}; H_p^1)$, we can estimate after integration

$$|u(\bar{t})|_{H^1}^2 + C\|\Delta u\|^2 \leq C\bar{t} \,,$$

and we have the desired result $u \in L^2(0, \bar{t}; H_p^2)$.

Similarly we test the heat equation (8b) by $-\Delta T$

$$\frac{1}{2}\frac{d}{dt}|u|_{H^1}^2 + c\|\Delta T\|^2 = K(u_t, \Delta T) \leq C(K, c)\|u_t\|^2 + \frac{c}{2}\|\Delta u\|^2$$

Using the bound on u_t, and integrating yields $T \in L^2(0, \bar{t}; H_p^2)$.

A usual limiting process (following e.g. [26], Chapter 3) yields global existence.

□

Theorem 2 (Uniqueness and continuous dependence on initial data)**.** *The solutions from Theorem 1 are uniquely defined and depend continuously on the initial data, assuming that the temperature stays below the critical temperature. In particular we then have*

$$\|u_1 - u_2\|_{H^1}^2 + \|T_1 - T_2\|_{H^1}^2 \leq C\left[\|u_1^0 - u_2^0\|_{H^1}^2 + \|T_1^0 - T_2^0\|_{H^1}^2\right] e^{Ct} \tag{26}$$

Proof. This can be seen by defining two solutions $(u_1, T_1), (u_2, T_2)$ and their difference $(w, v) = (u_1 - u_2, T_1 - T_2)$ that leads to the weak system

$$(w_t, \varphi) = \varepsilon(\Delta_w w, \varphi) - \frac{1}{\varepsilon}(W_u(u_1; m_1) - W_u(u_2; m_2), \varphi) \,, \tag{27}$$

$$(v_t, \psi) = c(\Delta v, \psi) + K(w_t, \psi) \,, \tag{28}$$

Testing with $(\varphi, \psi) = (w, v)$ yields

$$\frac{1}{2}\frac{d}{dt}\|w\|^2 = -\varepsilon|w|_B^2 - \frac{1}{\varepsilon}(W_u(u_1; m_1) - W_u(u_2; m_2), u_1 - u_2) \,, \tag{29}$$

$$\frac{1}{2}\frac{d}{dt}\|v\|^2 = -c|\nabla v|^2 + K(w_t, v) \,, \tag{30}$$

Assume for now that both solutions u_i are in $L^\infty(L^\infty)$, then for m_i the polynomials $W_u(u_i, m_i)$ are Lipschitz and we can choose a jointly working constant for any T. Hence we conclude with the estimate

$$\frac{1}{2}\frac{d}{dt}\left(\|w\|^2 + \|v\|^2\right) + \varepsilon|w|_B^2 + c|v|_{H^1}^2 \leq C\|w\|^2 + K\int w_t v dx \tag{31}$$

Testing the phase field equation with $\varphi = w_t$ and the temperature equation with $-\Delta v$ yields additionally

$$\|w_t\|^2 + \varepsilon\frac{d}{dt}|w|_B^2 = -\frac{1}{\varepsilon}\int (W_u(u_1; m_1) - W_u(u_2; m_2))w_t \leq C\|w\|\|w_t\|$$

$$C_1\frac{d}{dt}\|\nabla v\|^2 + C_2\|\Delta v\|^2 \leq \frac{1}{4}\|w_t\|^2 .$$

Adding these up yields

$$\frac{1}{4}\|w_t\|^2 + \frac{d}{dt}\left[\varepsilon|w|_B^2 + C_1\|\nabla v\|^2\right] \leq C\|w\|^2$$

Together with estimate (31) we conclude

$$\frac{1}{2}\frac{d}{dt}\left(\|w\|^2 + 2\varepsilon|w|_B^2 + \|v\|^2 + 2C_1\|\nabla v\|^2\right) + \varepsilon|w|_B^2 + c|v|_{H^1}^2 \leq C\|w\|^2 + \frac{K^2}{2}\|v\|^2$$

This applies for Gronwall which now states

$$\|w\|^2 + 2\varepsilon|w|_B^2 + \|v\|^2 + 2C_1\|\nabla v\|^2 \leq C\left[\|w^0\|^2 + |w^0|_B^2 + \|v^0\|_{H^1}^2\right]e^{Ct}$$

In particular we can use the equivalence of the Besov semi-norm and constant estimation to conclude with assertion (26). However, it remains to be shown that $u_i \in L^\infty(0, \bar{t}; L_p^\infty)$. Therefore we show that any solution is in $L^\infty(0, \bar{t}; H_p^2)$ which yields the assertion as for dimension $n \leq 3$ Sobolev's embedding theorem gives the right embedding.

Hence show that for any $\bar{t} : \|u(\bar{t})\|_{H^2} \leq C$: Testing (on the Galerkin level) the phase field equation by $-\Delta u_t$ yields

$$\begin{aligned}
(u_t, -\Delta u_t) + \varepsilon\mathcal{B}(u, \Delta u_t) &= \frac{1}{\varepsilon}(W_u(u; m), \Delta u_t) \\
\Rightarrow \|\nabla u_t\|^2 + \varepsilon\frac{d}{dt}|\nabla u|_B^2 &\leq -C(\nabla W_u(u; m), \nabla u_t) \\
&= -C\int W_{uu}(u; m)\nabla u\nabla u_t + W_{um}(u; m)\nabla m\nabla u_t dx \\
&\leq C\int |\nabla u||\nabla u_t| + |\nabla m||\nabla u_t| dx \\
&\leq \frac{1}{2}\|\nabla u_t\|^2 + C(\|\nabla u\|^2 + \|\nabla m\|^2) .
\end{aligned}$$

Furthermore we have under the temperature assumption

$$\|\nabla m\|^2 = \int |\nabla m|^2 dx = C\int \frac{|\nabla T|^2}{(1 + c_2(T_e - T))^2} \leq C\|\nabla T\|^2$$

so that we estimate overall, after integration and using the yet established bounds,

$$\frac{1}{2}\int_0^{\bar{t}} \|\nabla u_t\|^2 dt + \varepsilon|\nabla u(\bar{t})|_B^2 \leq C$$

and hence due to the equivalence of the semi-norms $u \in L^\infty(0, \bar{t}; L_p^\infty)$.

□

Remark In the proof we have used that the temperature stays below the critical temperature (slightly above would be fine, too) and this assumption demands that the initial temperature profile is also below this value.

4 Numerical methods and comparisons

The simulations are carried out with a pseudospectral method for both equations, the classical model and its wavelet analogue. While definition of Δ_w suggests a natural discretisation in wavelet space, we use a Fourier spectral method for the heat equation, using Fourier modes for 1-periodic functions in both spatial directions. In terms of these expansions, the system is written as the following system of ODEs

$$\sum_{j=0}^{N}\sum_{\mathbf{k}\in\mathbb{Z}_j^2}\sum_{\psi\in\Psi}(w_{j,\mathbf{k},\psi})_t\psi_{j,\mathbf{k}} = \varepsilon\sum_{j=0}^{N}\sum_{\mathbf{k}\in\mathbb{Z}_j^2}\sum_{\psi\in\Psi}-2^{2j}w_{j,\mathbf{k},\psi}\psi_{j,\mathbf{k}} + \sum_{j=0}^{N}\sum_{\mathbf{k}\in\mathbb{Z}_j^2}\sum_{\psi\in\Psi}c_{j,\mathbf{k},\psi}\psi_{j,\mathbf{k}}$$

$$\sum_j(\hat{T}_j)_t\exp(ijx2\pi) = \sum_j -j^2 4\pi^2\hat{T}_j\exp(ijx2\pi) + K\sum_j(\hat{\xi}_j)_t\exp(ijx2\pi)\,.$$

The coefficients $c_{j,\mathbf{k},\psi}$ are related to the third order polynomial $\mathcal{W}[u(1-u)(u-\frac{1}{2}+m)]$ by a stationary wavelet transform and the Fourier coefficients $\hat{\xi}_j$ are determined by transforming $\sum_{j=0}^{N}\sum_{\mathbf{k},\psi\in\Psi}(w_{j,\mathbf{k},\psi})_t\psi_{j,\mathbf{k}}$ into discrete Fourier space. We discretise in time by a semi-implicit Euler scheme that treats the linear parts implicitly,

$$\frac{w^+_{j,\mathbf{k},\psi}-w_{j,\mathbf{k},\psi}}{dt} = -2^{2j}w^+_{j,\mathbf{k},\psi} + c_{j,\mathbf{k},\psi} \tag{32a}$$

$$\frac{\hat{T}^+_j-\hat{T}_j}{dt} = -j^2 4\pi^2\hat{T}^+_j + K\hat{\xi}_j\,, \tag{32b}$$

where the $+$ superscript indicates the new, updated coefficients. We employ convexity splitting to gain stability which is reflected in the update, too (see below). We update the wavelet coefficients first and then use the resulting approximation for u_t to calculate the coefficients $\hat{\xi}_j$. Also note that the $c_{j,\mathbf{k},\psi}$ in (32a) are evaluated using the coefficients of the temperature approximations $\hat{T}_j$ at the old time level.

The update for the temperature is rather standard for spectral methods. For the order parameter, however, we want to go into more detail. The stationary wavelet transform yields four fields for the scaling function coefficients A, and H, V, D for the horizontal, vertical and diagonal wavelet coefficients, respectively. In MATLAB with the corresponding ordering, to calculate the wavelet Laplacian we multiply the jth scale by $2^{2(N-j)}$. For the jth coefficient level, let $R_j \in \{A_j, H_j, V_j, D_h\}$ be one of the coefficient arrays, and $R_{3,j}$ the same kind of coefficients for the cubic expression, then we update, with the convexity splitting parameter C,

$$R_j = \frac{R_j + dt/\tau(R_{3,j} + dtCR_j)}{1 + dt(2^{2(N-j)}\varepsilon/\tau + C)}\,.$$

4.1 Limiting case: Allen-Cahn model

Before we investigate numerically the evolution of the new model and compare it with the classical recrystallisation model, it is instructive to first probe the models

in a simpler setting, and consider a special case where the models introduced in section 2 reduce to scalar Allen-Cahn type equations. Specifically, we set the latent heat parameter $K = 0$ and let the initial temperature field to be uniform, $T(x, 0) = T_c$, where T_c is a non-negative constant. For Kobayashi's original model (2)-(6), we obtain the anisotropic Allen-Cahn equation

$$u_t = -\frac{\delta}{\delta u}\mathcal{E}(u; \varepsilon, A) = \varepsilon\nabla \cdot \big(\gamma(\theta)\gamma'(\theta)\nabla^{\perp}u\big) + \varepsilon\nabla \cdot \big(\gamma(\theta)^2\nabla u\big) - \frac{1}{\varepsilon}W'(u)\,, \tag{33}$$

where $\nabla^{\perp}u = (-u_y,\, u_x)^T$ is the orthogonal gradient. The new model (8) with (2), (6) reduces to the "wavelet Allen-Cahn equation",

$$u_t = \varepsilon\Delta_w u - \frac{1}{\varepsilon}W'(u). \tag{34}$$

All of the above are L^2 gradient flows of the corresponding free energies i.e. (1)-(3) with $\delta = 0$ for the isotropic Allen-Cahn model , $\delta > 0$ for the anisotropic Allen-Cahn model and (7) as appropriate.

Moreover, we set the temperature to be at equilibrium, $T_c = T_e$, then $m = 0$ and the homogeneous free energy contribution is symmetric,

$$W(u) = \frac{1}{4}u^2(u-1)^2. \tag{35}$$

In all numerical results in this section, the initial condition for u was a small random perturbation of of $u = 1$.

In Figure 1 (a)-(c) we observe the well-known emergence of a coarsening pattern for the Allen-Cahn equation, that coarsens independent of the direction of the wave number as seen from the corresponding two-dimensional Fourier spectra (a')-(c'), as expected for an isotropic pattern.

Figure 2 (a)-(c) shows the evolution for the classical anisotropic Allen-Cahn equation for the choice of $n = 4$ and $\delta = 0.065$ so that the anisotropy is still in the weak regime. The resulting patterns are similar as for the isotropic case in the early phase of evolution, but at later stages as domains in the pattern have grown show a directional dependence that is in accordance with a four-fold symmetry for γ, and shown in the corresponding Fourier spectrum (a')-(c').

We now carry out a numerical study to investigate the emergence of anisotropy and its long-time evolution in the Wavelet-Allen-Cahn equation. As has been shown in [9], volume constrained minimisers of the free energy using the Besov semi-norm lead to Wulff shapes with a clear four-fold symmetry for the new Wavelet-Allen-Cahn equation. Using the stationary wavelet transform has a similar effect as differencing in Fourier space: periodic boundary conditions are fulfilled intrinsically. Figure 3 (a) - (c) depicts a typical evolution that compares well to the numerical results for the anisotropic Allen-Cahn equation (33). The white and black regions correspond to the order parameter being approximately 0 or 1. Coarsening takes place in a similar fashion as for the classical anisotropic Allen-Cahn model. The Figures (a')-(c') show the absolute values of the Fourier transforms corresponding to the patterns in (a)-(c). One clearly sees the emergence of the anisotropic four-fold symmetry in the pattern.

In Figure 4 we show for all three cases a coarsening diagram for the runs with the same parameters as above, shown in a doubly logarithmic plot. We calculated the

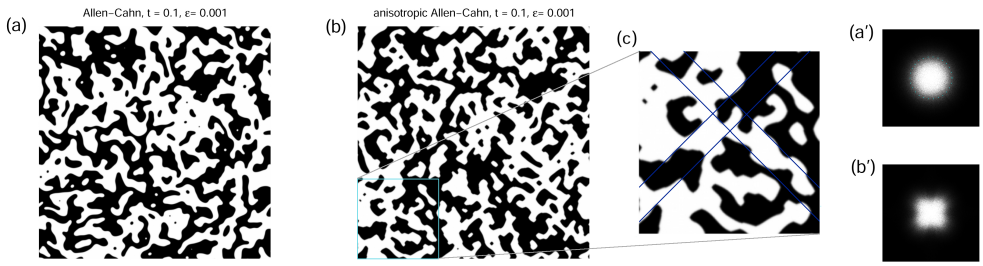

Figure 1: Numerical results for the isotropic Allen-Cahn model ($\delta = 0$) for $\varepsilon = 0.001$ on a 1024$\times$1024 grid at three different times, $t = 0.01, t = 0.1, t = 1$; (a'), (b') and (c') show the absolute values of the two-dimensional discrete Fourier transform, corresponding to (a), (b) and (c), respectively.

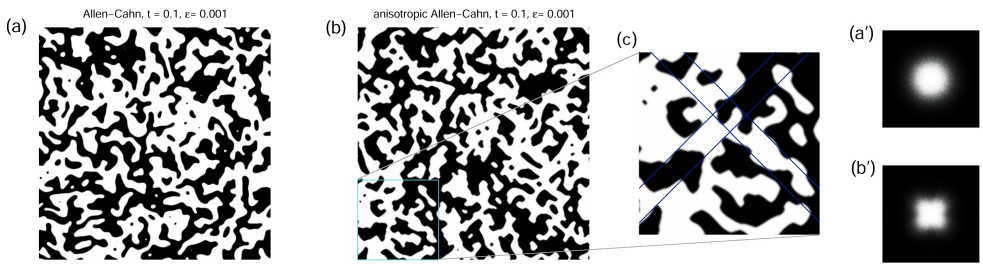

Figure 2: Numerical results for the anisotropic Allen-Cahn model for $\varepsilon = 0.001$ on a 1024$\times$1024 grid with anisotropy $\delta = 0.065$ at three different times, $t = 0.01, t = 0.1, t = 1$; (a'), (b') and (c') show the absolute values of the two-dimensional discrete Fourier transform, corresponding to(a), (b)and (c), respectively, showing the evolution towards anisotropic pattern.

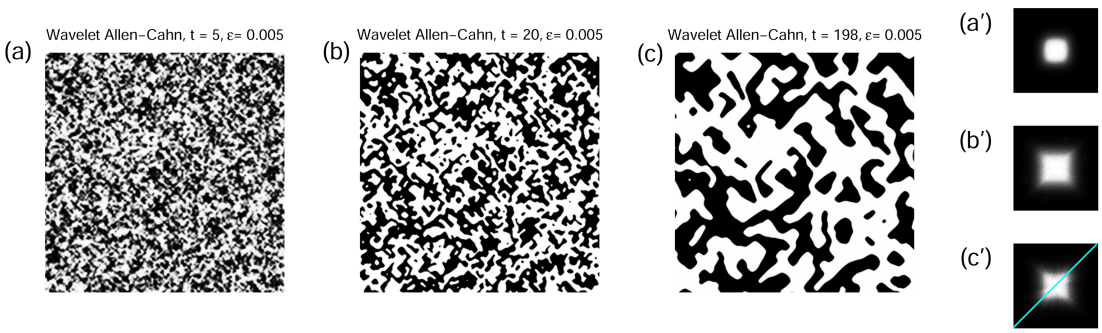

Figure 3: Numerical results for the Wavelet-Allen-Cahn model for $\varepsilon = 0.005$ (why not $\varepsilon = 0.001$?) on a 1024$\times$1024 grid for a unitary domain at three different times $t =???$. (a'), (b') and (c') are the absolute values of the two-dimensional discrete Fourier transform, corresponding to (a), (b) and (c), respectively.

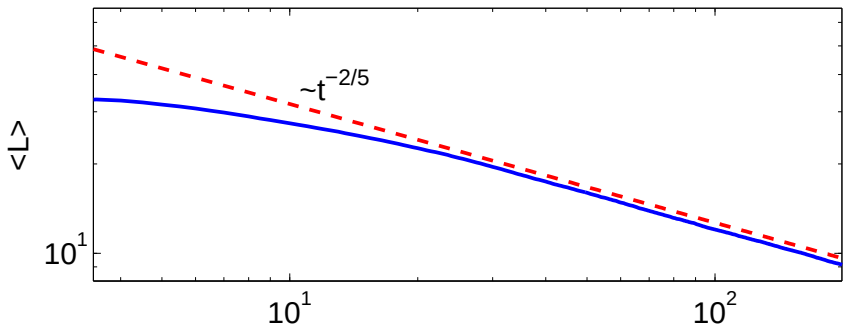

Figure 4: Coarsening diagram for the isotropic Allen-Cahn, anisotropic Allen-Cahn and the Wavelet-Allen-Cahn for $\varepsilon = 0.005$ on a 1024×1024 grid. Time vs $< L >= \sum_{i=1}^{n_y} N_i/n_y$, where n_y is the number of grid points in vertical direction and N_i is the number of phases in the corresponding one-dimensional (parallel to the x-axis) sheet. Dashed curve: $\sim t^{-2/5}$ the Wavelet-Allen-Cahn equation.

number of domains for each cross-section parallel to the x-axis and divided by the number of these layers - the number of grid points in the y-direction, which yields a measure for the typical length scale

$$\langle L \rangle = \sum_{i=1}^{n_y} N_i(t)/n_y.$$

The numerical results show that the approach is according to a power law behaviour $\langle L \rangle \sim t^{-2/5}$, for the isotropic Allen-Cahn, and eventually $\langle L \rangle \sim t^{-2/5}$ for the anisotropic Allen-Cahn as $t \to \infty$. From the simulations one can conclude from the comparisons of the classical anisotropic Allen-Cahn equation and the Wavelet-Allen-Cahn equation, that while the approach to the Wulff-shape occurs on different time scales that arises from the different scalings of both models, the coarsening rate remains the same.

4.2 Recrystallisation with thermal coupling

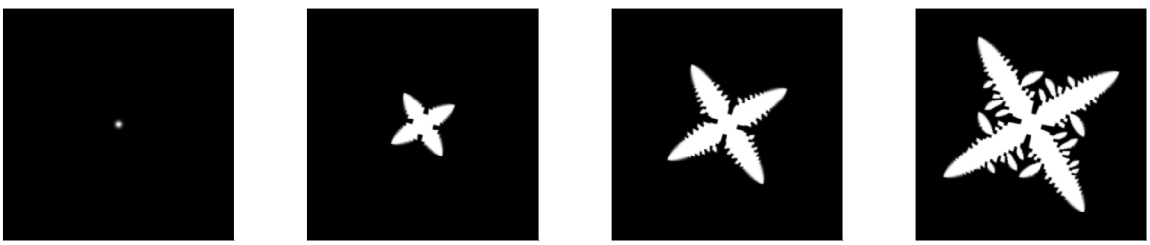

Figure 5: Numerical results for Kobayashi's model, (4) and (5), using γ as in (36) with $\delta = 0.15$.

While for the Wavelet-Allen-Cahn case we have used small scaled random noise as initial conditions, here we instead insert a very narrow Gaussian into the domain as

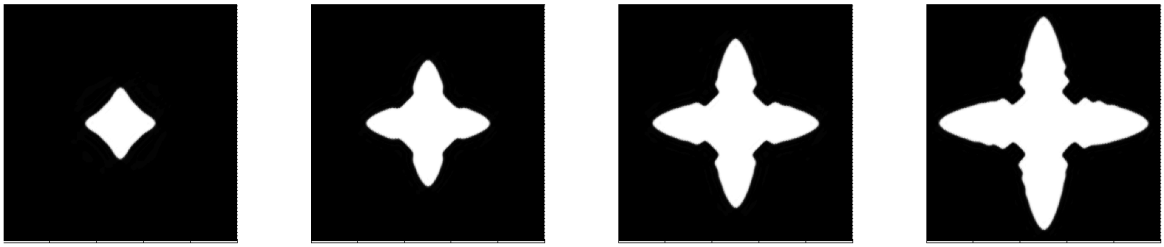

Figure 6: Dendritic growth based on the intrinsic anisotropy of the Wavelet-Laplacian.

a nucleation site to start the recrystallisation process, in fact similar to what happens in physical experiments. For comparison we note first a recent study [1] on numerical methods and conditions regarding the accurate numerical description of dendritic patterns. For our numerical implementation of the original model by Kobayashi, we show for the system (5) and (4) with

$$\gamma(\theta) = 1 + \delta \cos(4(\theta + \pi/6)) \tag{36}$$

As expected, the Figures 5-6 show that the growing nucleus develops a branching structure that becomes more pointed as δ is increased. In addition, the branches align more closely with the horizontal and vertical directions, reflecting the increasingly stronger degree to which the four-fold symmetry is imposed by γ and give good comparisons to the results in the literature as discussed in [1].

For the new model using the wavelet Laplacian we show in Figure 6 numerical results for one nucleus, a Gaussian, put into a square domain. Again, we see that the nucleus grows and exhibits faster growth in four preferred directions aligned with the axes. In fact, comparing the results from the wavelet based model with the classical model by Kobayashi for $\delta = 0.15$, we see that the preferential directions for the dendritic are well defined in both cases, suggesting that the anisotropy arises from the two different mechanisms are of similar strength with this choice of δ.

Hence we are indeed able to describe dendritic growth with the new derivative-free approach and its intrinsic anisotropic properties. However, the dendrites for the wavelet-based approach appear to have more rounded features.

5 Conclusions and outlook

This work explores the possibility of using the anisotropic nature of wavelet analogue of differential operators for mathematical models in anisotropic pattern formation in material science. For a standard model for dendritic crystal growth we have shown that a straightforward modification of the underlying free energy with a wavelet-based Besov instead of the H^1 semi-norm representation for the interface contribution, and hence replacing the Laplacian in the Ginzburg-Landau formulation of the phase-field evolution, produces a four-fold symmetry of the preferred growth directions.

In contrast, Kobayashi's original model required an explicit dependence of the surface tension coefficient on the solution gradient to obtain anisotropy, thus leading to a

quasi-linear PDE for the phase-field whereas the wavelet-based model has a linear, derivative free operator with an intrinsic anisotropy.

All our results thus confirm that the behaviour reflects the symmetry suggested in [9], and compare well to the evolution as well as the long-time rates of change of the patterns known from the classical models.

Moreover, we found that the new formulation lends itself naturally to numerical solutions via wavelet or hybrid e.g. wavelet-spectral methods and complexity splitting where the implicit terms are linear. The resulting scheme is easily implemented in MATLAB with the help of the available wavelet tools.

We also note, that the model is easily generalised to 3D and in fact our well-posedness result applies also to this case, and it would be interesting to see if an efficient implementation is possible that would be competitive with existing simulations.

There are, of course, a number of open problems and directions for future research. In particular to extend our investigations to surface energies to other four- or eight-fold symmetries. This may require generalisations to other wavelets or other generalisations such as for example shearlets.

Acknowledgment

The authors thank Andrea Bertozzi for helpful comments and Dirk Peschka for sharing his valuable insights into anisotropic phase separation.

A Wavelet construction

A general introduction to wavelets in different settings can be found in many references, e.g. [6, 7, 18]. We denote the mother wavelet by ψ and the scaling function by ϕ. The tensor product ansatz leads to the basis functions

$$\begin{aligned} \psi^d(x,y) &= \psi(x)\psi(y), \quad \psi^v(x,y) = \psi(x)\phi(y), \\ \psi^h(x,y) &= \phi(x)\psi(y), \qquad \phi(x,y) = \phi(x)\phi(y). \end{aligned}$$

By $\tilde{\Psi} = \{\psi^d, \psi^v, \psi^h\}$ we denote the set of diagonal, vertical and horizontal components. For $j \in \mathbb{Z}$, $\mathbf{k} \in \mathbb{Z}^2$, $\psi \in \tilde{\Psi}$ we define the wavelet mode

$$\psi_{j,\mathbf{k}} = 2^j \psi(2^j \mathbf{x} - \mathbf{k}),$$

and similarly

$$\phi_{j,\mathbf{k}} = 2^j \phi(2^j \mathbf{x} - \mathbf{k}).$$

Every f can be written as

$$f = \sum_{j,\mathbf{k},\psi \in \tilde{\Psi}} w_{j,\mathbf{k},\psi} \psi_{j,\mathbf{k}}$$

with

$$w_{j,\mathbf{k},\psi} = \int f(\mathbf{x})\psi_{j,\mathbf{k}} d\mathbf{x}\,. \tag{37}$$

Given such an expression of f the wavelet Laplace operator is defined as [8–10]

$$\Delta_w f = \sum_{j,\psi} -2^{2j} \int (f, \psi_{j,\mathbf{k}})\psi_{j,\mathbf{k}} d\mathbf{k}\,. \tag{38}$$

On a finite domain $[0,1]^2$ one uses $j \in \mathbb{N}_{\geq 0}$ and $k_l = 0, 1, \ldots, 2^j, l = 1, 2$, as the spatial shifts make only sense as long as the support of the wavelets is still inside the domain. The resulting set of $\boldsymbol{k}$ is denoted by $\mathbb{Z}_j^2$. Notice also that numerical applications require finite sums and therefore we incorporate the scaling function to represent non-zero contributions to the average of f, which play a similar role as the constant mode in a Fourier expansion. Thus, we extend the set $\Psi = \tilde{\Psi} \cup \{\phi\}$ and write f as

$$f = \sum_{j=0}^{N} \sum_{\mathbf{k}\in\mathbb{Z}_j^2} \sum_{\psi\in\Psi} w_{j,\mathbf{k},\psi}\psi_{j,\mathbf{k}}\,.$$

Then, approximations to the coefficients in (37) as well as the Besov semi-norm (**??**) and the wavelet Laplacian (38) are given through finite sums instead of integrals. Coefficients for $\phi_{j,\boldsymbol{k}}$ are defined in the same fashion as for the $\psi_{j,\boldsymbol{k}}$.

References

[1] J. W. Barrett, H. Garcke, and R. Nürnberg. Stable Phase Field Approximations of Anisotropic Solidification. *arXiv:1210.6791*, 2013.

[2] A. Braides. *Gamma-Convergence for Beginners*. Oxford University Press, 2002.

[3] E. Burman and J. Rappaz. Existence of solutions to an anisotropic phase-field model. *Math. Meth. Appl. Sci.*, 26:1137–1160, 2003.

[4] W. K. Burton, N. Cabrera, and F. C. Frank. The Growth of Crystals and the Equilibrium Structure of their Surfaces. *Phil. Trans. R. Soc. Lond. A*, 243(866):299–358, 1951.

[5] C. Cattani. Harmonic wavelets towards the solution of nonlinear PDE. *Comp. Math. Appl.*, 50(8-9):1191–1210, 2005.

[6] W. Dahmen. Wavelet and Multiscale Methods for Operator Equations. *Acta Num.*, 6:55–228, 1997.

[7] I. Daubechies. *Ten lectures on wavelets*. SIAM, Philadelphia, PA, USA, 1992.

[8] J. A. Dobrosotskaya and A. L. Bertozzi. A Wavelet-Laplace Variational Technique for Image Deconvolution and Inpainting. *IEEE Trans. Imag. Proc.*, 17(5):657–663, 2008.

[9] J. A. Dobrosotskaya and A. L. Bertozzi. Wavelet analogue of the Ginzburg-Landau energy and its Gamma-convergence. *Interf. Free Boundaries*, 12(2):497–525, 2010.

[10] J. A. Dobrosotskaya and A. L. Bertozzi. Analysis of the Wavelet Ginzburg-Landau Energy in Image Applications with Edges. *SIAM J. Imaging Sci.*, 6(1):698–729, 2013.

[11] M. E. Glicksman. *Principles of Solidification*. Springer, 2011.

[12] C. Herring. Some theorems on the free energies of crystal surfaces. *Phys. Rev.*, 82(1):87–93, 1951.

[13] M. Holmström. Solving Hyperbolic PDEs Using Interpolating Wavelets. *SIAM J. Sci. Comput.*, 21(2):405–420, 1999.

[14] M. Holmström and J. Waldén. Adaptive Wavelet Methods for Hyperbolic PDEs. *J Sci. Comp.*, 13(1):19–49, 1998.

[15] L. Jameson. A Wavelet-Optimized, Very High Order Adaptive Grid and Order Numerical Method. *SIAM J. Sci. Comput.*, 19(6):1980–2013, 1998.

[16] A. Karma and W.-J. Rappel. Numerical Simulation of Three-Dimensional Dendritic Growth. *Phys. Rev. Lett.*, 77(19):4050, 1996.

[17] R. Kobayashi. Modeling and numerical simulations of dendritic crystal growth. *Physica D*, 63, 1993.

[18] S. Mallat. *A Wavelet Tour of Signal Processing, Third Edition: The Sparse Way*. Academic Press, 2008.

[19] K. Schneider and O. V. Vasilyev. Wavelet Methods in Computational Fluid Dynamics. *Ann. Rev. Fluid Mech.*, 42(1):473–503, 2010.

[20] I. Steinbach. Phase-field models in materials science. *Mod. Sim. Mater. Sci. Eng*, 17(7):073001, 2009.

[21] O. V. Vasilyev and S. Paolucci. A Fast Adaptive Wavelet Collocation Algorithm for Multidimensional PDEs. *J. Comp. Phys.*, 138:16–56, 1997.

[22] O. V. Vasilyev, S. Paolucci, and M. Sen. A Multilevel Wavelet Collocation Method for Solving Partial Differential Equations in a Finite Domain. *J. Comp. Phys.*, 120:33–47, 1995.

[23] S.-L. Wang, R. F. Sekerka, A. A. Wheeler, B. T. Murray, S. R. Coriell, R. J. Braun, and G. B. McFadden. Thermodynamically-consistent phase-field models for solidification. *Physica D*, 69:189–200, 1993.

[24] A. A. Wheeler, B. T. Murray, and R. J. Schaefer. Computation of dendrites using a phase field model. *Physica D*, 66(243), 1993.

[25] G. Wulff. Zur Frage der Geschwindigkeit des Wachstums und der Auflösung der Krystallflächen. *Zeitschrift f. Krystall. Mineral.*, 34:449–530, 1901.

[26] S.-M. Zheng. *Nonlinear Evolution Equations*. Pitman series Monographs and Survey in Pure and Applied Mathematics 133, Chapman Hall/CRC, Boca Raton, Florida, 2004.